IEEE Access
Multidisciplinary | Rapid Review | Open Access Journal

Received August 5, 2021, accepted October 14, 2021, date of publication October 26, 2021, date of current version November 15, 2021.

Digital Object Identifier 10.1109/ACCESS.2021.3123256

An Integrated Design Based on Dual Thresholding and Features Optimization for White Blood Cells Detection

JAVARIA AMIN[1], MUHAMMAD SHARIF[2], (Senior Member, IEEE), MUHAMMAD ALMAS ANJUM[3], MUSSARAT YASMIN[2], KHALID IQBAL KHATTAK[2], SEIFEDINE KADRY[4], (Senior Member, IEEE), AND SANGHYUN SEO[5]

[1]Department of Computer Science, University of Wah, Wah Cantt 47040, Pakistan
[2]Department of Computer Science, COMSATS University Islamabad, Wah Campus, Wah Cantt 47040, Pakistan
[3]National University of Technology (NUTECH), Islamabad 44000, Pakistan
[4]Department of Applied Data Science, 4612 Kristiansand, Norway
[5]College of Art and Technology, Chung-Ang University, Anseong 06974, Republic of Korea

Corresponding authors: Muhammad Sharif (muhammadsharifmalik@yahoo.com) and Sanghyun Seo (sanghyun@cau.ac.kr)

This work was supported in part by the National Research Foundation of Korea (NRF) Grant by the Korean Government through Ministry of Science and ICT (MSIT) under Grant 2019R1F1A1058715, and in part by the Chung-Ang University Research Scholarship Grants, in 2021.

ABSTRACT White blood cells (WBC) are an important component of immune mechanism, as they protect human body from parasites, viruses, fungi, and bacteria. The number of blood cells provides significant information related to infections such as AIDS, leukemia, deficiencies of immune and autoimmune infections. To heal an infection in a timely manner, it is critical to recognize it early on. Therefore, a method is proposed to accurately segment and classify WBC at an early stage. The RGB image is converted into HSV after which dual thresholding is applied to the saturation component to segment WBC. The 1000 features are extracted from Alexnet to FC8 layer, Logits layer is selected for feature extraction from mobilenetv2, node_202 layer is utilized to extract the features from shuffle net and FC1000 layer is chosen from Resnet-18 model. Four feature vectors are obtained from transfer learning models; these feature vectors are combined serially and create the final optimized vector by non-dominated sorting genetic algorithm (NSGA). The classification results are investigated on the fusion of Alexnet, shuffle net, Resnet-18, mobilenetv2 and the fusion of mobilenetv2, shuffle net and Resnet-18 whereas mobilenetv2 features are fused independently. The method is tested on three publicly available datasets such as LISC, ALL_IDB1, and ALL_IDB2. The method achieved maximum 1.00 accuracy to classify the blast/non-blast cells, 0.9992 accuracy on Basophil cells, and 1.00 accuracy on Lymphocyte, Neutrophil, Monocyte, Eosinophil, and mixture of these cells. When compared to existing modern approaches, the proposed method produces better outcomes.

INDEX TERMS Thresholding, deep features, fusion, HSV, leukemia.

I. INTRODUCTION

The human body contains three types of cells named as white, red and platelets. White cells are part of immune systems, known as immune cells [1]. These cells provide protection to the body from different kinds of infectious disorders [2]. White cells are initiated from the red marrow of bone except few from vital body glands. These cells are colorless; therefore hematologists might utilize stains to visualize them under a microscope. Several diseases occur due to the irregular range of WBC types (Lymphocytes, Eosinophils, Neutrophils and Monocytes) [3]. These types of blood cells are helpful to diagnose blood related diseases [4]. Leukemia is a blood cancer when abnormal cells of white platelets are grown rapidly in bone marrow as shown in Figure 1. The uncontrolled growth of white platelets destroys the body's immune system [5].

The immune system provides protection against ailments. The number of white cells is increased due to imbalanced cell structure leading to cancer development known as Leukemia [7]. Hematologists must manually detect and classify blood cells, which really is laborious & time-consuming [8].

Therefore, an automated method for blood cells detection/classification helps hematologists for the diagnosis of

The associate editor coordinating the review of this manuscript and approving it for publication was Gangyi Jiang.

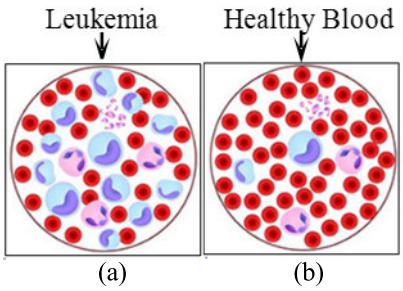

FIGURE 1. Blood cells (a) Leukemia (a) Healthy blood [6].

abnormal cells at an early stage [9]. If aberrant cell growth is found early on, it may improve the patient's chances of survival [10]. In literature, although much work has been done for the detection of abnormality in blood cells, still there is a gap for improvement to detect the blood cells abnormality more accurately [11]–[13]. This research work accurately segments WBC and classifies its different types using deep features. The following is the key contribution:

1) RGB images are transformed into HSV color space. The dual thresholding approach is applied to the saturation component for the segmentation of WBC and morphological operations are utilized to refine the segmentation with a specific structuring element.
2) Deep features are extracted using convolutional neural networks (CNN), fused serially and optimized through NSGA. The optimized feature vector is passed to different classifiers.

II. RELATED WORK

In literature, a variety of work has been done for Leukemia detection based on machine learning that is discussed in this section. Otsu thresholding approach with HSV color spaces is used for blood cells segmentation [14]. Golden Section Search (GSS) approach is used to select optimum threshold value applied to Hue component for segmentation [15]. The iterative thresholding [16] technique is applied on different components of color spaces [17] for accurate leukocytes segmentation [18]. Cytoplasm is extracted using region growing approaches [19]. The global threshold with morphological opening methods is utilized to segment leukemia in microscopic images [20]. SVM [21], [22], [24], [25], KNN, Probabilistic neural network (PNN), is used to identify blood cells [23] using chromatic, textural, and geometrical information [24]–[26]

The shape-based features such as contour signature and Hausdorff Dimension are utilized for the detection of Leukemia [27]. The features reduction methods of PCA and Probabilistic PCA (PPCA) are used to optimize feature vector [28]. The clustering approaches such as Nature-Inspired Optimization (NIO) [29], Particle Swarm Optimization (PSO) [30], Artificial Fish (AF) swarm [29], Quantum Genetic with fuzzy c means (FCM) [31], Levy flight PSO (LPSO) [32], Pulse-Coupled Neural Network (PCNN) [33], Mean Shift Clustering (MSC) and FCM [34] are made use of to accurately segment the required region of interest (ROI). In the last decade, deep learning (DL) approaches are used almost in all kinds of applications. DL processes input images directly. In CNN, different size of filters is used to learn complicated patterns [35]–[40]

III. PROPOSED METHODOLOGY

The proposed approach classifies different types of WBC. There are three primary steps in the approach. The initial step is to study several color spaces in order to choose the best color space for better segmentation results. The blood cells are segmented using global thresholding [41] in the segmentation process. Distinct transfer learning models are fed segmented images to classify blood cells into different classifications. A brief overview of proposed methodology is illustrated in Figure 2.

A. PREPROCESSING

The color space represents the colors in a geometrical manner. Colors are specified through three main components and numerical values represent explicit color. The values of Hue are varied from 0 to 1. When Hue values increase, transitions of color appear in red to orange, cyan, green, magenta, yellow and back to red. In saturation, 0 denotes neutral and 1 shows maximum value of saturation. In NTSC color space [42], luminance component represents the gray signal in a monochrome i.e., white/black and other components contain information related to hue saturation in which 0 denotes empty component and 1 represents full components of saturation. YCbCr contains Y luminance and Cb and Cr chrominance channels. For the selection of appropriate color space, RGB image is converted into HSV, YCbCr, and NTSC as shown in Figure 3. After conversion, it is observed that saturation component of HSV color space presents nuclei region more prominent. Therefore, saturation channel is selected for the segmentation of WBC. In HSV [43], one channel denotes brightness values but two-channel provides information related to color. The darkest cell regions are related to the nuclei. The nuclei and cytoplasm region is more clear in HSV color space which is mathematically denoted in Eq. 1-2 and Figure 4.

$$H = \begin{cases} 0 \\ \quad \text{if Maximum} = \text{Minimum} \\ \quad \leftrightarrow \text{Red} = \text{Green} = \text{Blue} \\ 60^{\circ}.\left(0 + \dfrac{\text{Green} - \text{Blue}}{\text{Maximum} - \text{Minimum}}\right), \\ \quad \text{if Maximum} = \text{Red} \\ 60^{\circ}.\left(0 + \dfrac{\text{Blue} - \text{Red}}{\text{Maximum} - \text{Minimum}}\right), \\ \quad \text{if Maximum} = \text{Green} \\ 60^{\circ}.\left(0 + \dfrac{\text{Red} - \text{Green}}{\text{Maximum} - \text{Minimum}}\right), \\ \quad \text{if Maximum} = \text{Blue} \end{cases} \tag{1}$$

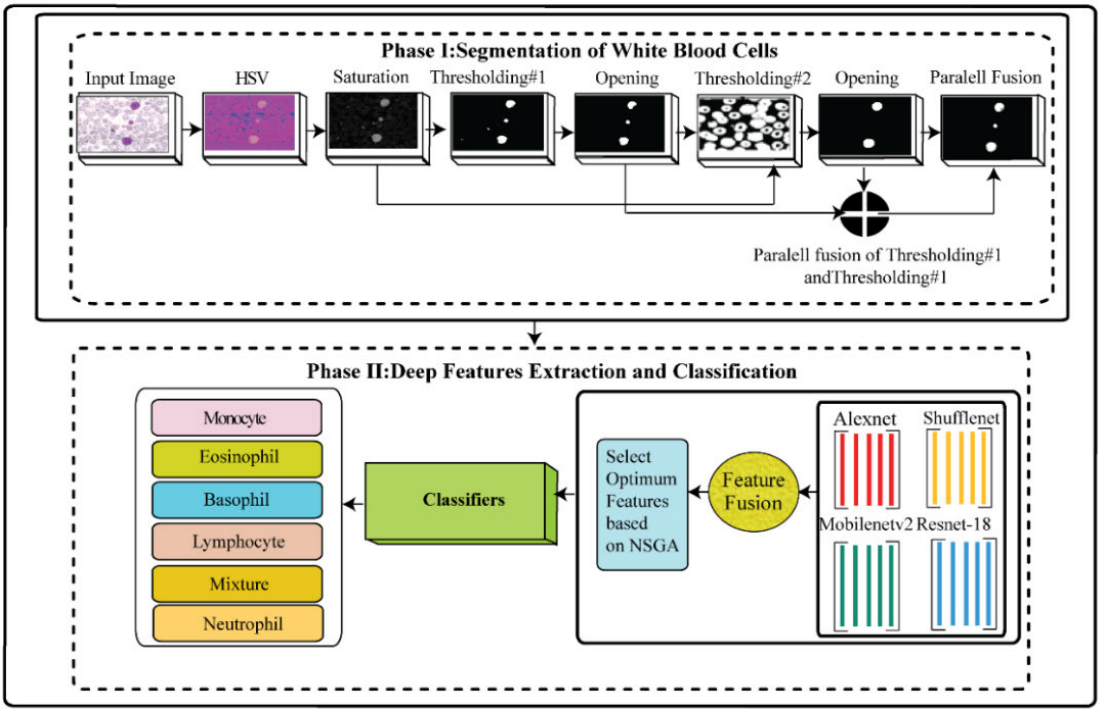

FIGURE 2. Dual thresholding for WBC segmentation and classification based on deep features fusion.

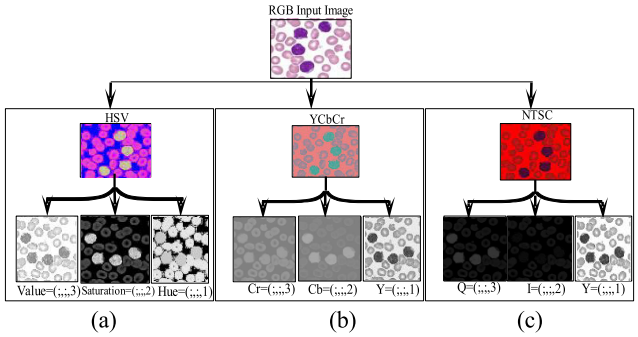

FIGURE 3. Nuclei information in different color spaces (a) HSV (b) YCbCr (c) NTSC (YIQ).

$$\text{if H} < 0^{\circ} \text{ then H:} = \text{H}+360^{\circ}$$

$$\text{S}_{\text{HSV}} = \begin{cases} 0, & \text{if Maximum} = 0 \leftrightarrow \text{Red} \\ & = \text{Green} = \text{Blue} \\ \dfrac{\text{Maximum} - \text{Minimum}}{\text{Maximum}}, & \text{otherwise} \end{cases} \tag{2}$$

B. WBC SEGMENTATION

In WBC, nucleus is the largest and most prognostic organ of cell whose accurate segmentation is a challenging task. Therefore, new method is proposed based on global thresholding for accurate segmentation of nucleus as well as cytoplasm.

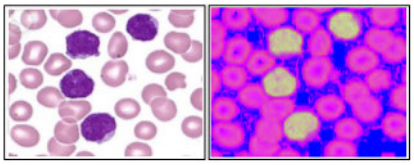

FIGURE 4. RGB to HSV conversion (a) input image in RGB (b) after conversion in HSV.

1) DUAL GLOBAL THRESHOLDING METHOD

The global threshold is better to define the degree of separation of intensity values among peaks of the image. In this method, global thresholding is applied to the saturation component separately two times named as dual global thresholding because single global threshold method only provides the nucleus or cytoplasm whereas both are necessary to segment WBC. Hence global thresholding methods provide better WBC segmentation after the fusion. The whole procedure is described below.

2) GLOBAL THRESHOLDING METHOD#1

The global thresholding method#1 is applied on the input images for WBC segmentation and mathematically expressed in Eq. 3 as:

$$\text{Global}_{\text{x,y}} = \begin{cases} 1 & \text{if } \text{S}_{\text{x,y}} \geq \text{Threshold} \\ 0 & \text{Otherwise} \end{cases} \tag{3}$$

where$\text{S}_{\text{x,y}}$ is the input image and $\text{Global}_{\text{x,y}}$ is the processed image after applying the threshold.

TABLE 1. Selection of optimal threshold value for global threshold method#1.

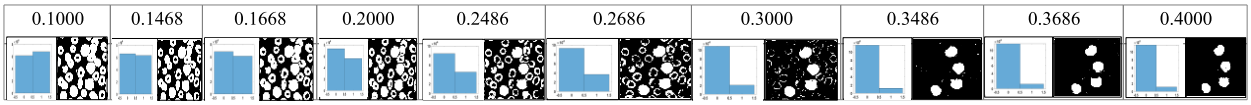

TABLE 2. Selection of optimal threshold value for global threshold method#2.

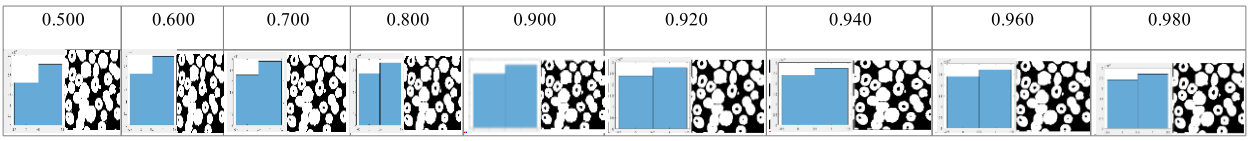

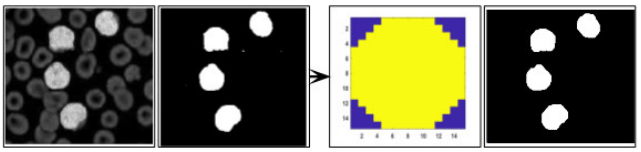

FIGURE 5. Blood cell segmentation (a) saturation component (b) global thresholding#1 (c) morphological opening with 8 disc shape structuring element.

Extensive experiments are performed for the selection of optimum threshold and results are presented in Table 1.

The experimentation is done with different threshold values while 0.3640 threshold value provided better segmentation results as compared with other threshold values as given in Table 1. Therefore, 0.3640 threshold is selected for global thresholding method#1 for segmentation. Furthermore, morphological operations are applied to refine the segmentation. The morphological opening is applied having 8 disk shape structuring element to remove imperfections and preserve the size/shape of the segmented image as shown in Figure 5. In this method, only nucleus region is segmented.

3) GLOBAL THRESHOLDING METHOD#2

The selection of optimum value of threshold is a challenging task. Thus experiments are done for the selection of optimal threshold value and results are presented in Table 2. In this experimentation, selected threshold values are greater than the previous threshold tested values used in method#1. This method provides whole segmented WBC but nucleus and cytoplasm regions are not differentiated.

Similarly the threshold value 0.960 is selected for global thresholding method#2 and applied to the saturation channel to segment WBC. A morphological opening having 28 structuring element is performed on segmented image by method#2 to refine the segmentation and visually shown in Figure 6.

4) PARALLEL FUSION OF DUAL THRESHOLDING APPROACH

Finally, WBC are more accurately segmented through the parallel fusion of segmented images obtained by global thresholding methods#1 and 2 as shown in Figure 7-8.

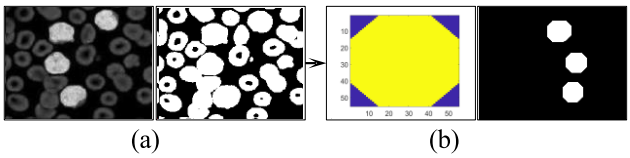

FIGURE 6. Cell segmentation (a) global threshold#2 (b) morphological opening with 28 structuring element.

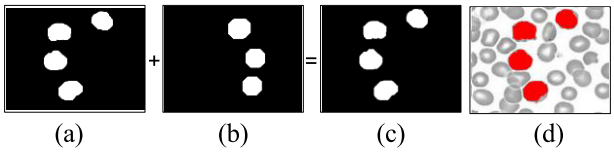

FIGURE 7. Dual thresholding results (a) global threshold#1 (b) global threshold#2 (c) parallel fusion of both global thresholding (d) mapping on input image.

When fusion is applied, nucleus and cytoplasm are clearly differentiated in segments of WBC. The visually and quantitative results in Figure 8 show that parallel fusion provides improved segmentation results because nucleus and cytoplasm are clearer after fusion.

In Figure 8, segmented region is also compared pixel by pixel with ground truth annotation. Figure provides two types of results to strengthen the claim. (i) Results are provided on the threshold values as well as on optimum selected threshold which can be seen in Row 1 and Row2 respectively as a sample in terms of dice score measure which shows that the selected optimal threshold value results are greater than the others threshold values, therefore 0.384 and 0.9600 threshold values are selected for methods#1 and 2 respectively. (ii) Similarly, dice score results of segmented images are measured using optimum threshold by methods#1 and 2 individually as well as after fusion of both segmented images by methods#1 & 2.

C. WBC CLASSIFICATION USING DEEP FEATURES

Machine learning is utilized widely for medical imaging analysis. The 1000 deep features are extracted through each transfer learning model such as Alexnet [44], ResNet-18 [45], mobilenetv2 [46], and shuffle net [47] with selected layer for

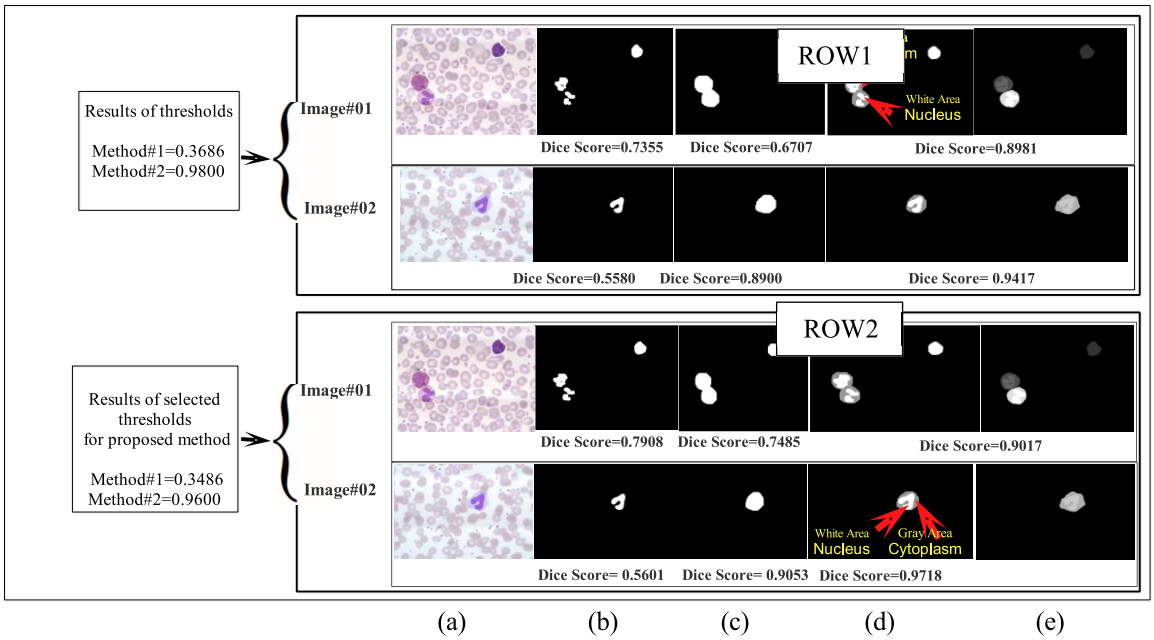

FIGURE 8. Segmentation experiment for selection of appropriate threshold value (a) input (b) thresholding method#1. (c) thresholding method#2 (d) parallel fusion of both thresholding methods (e) ground truth.

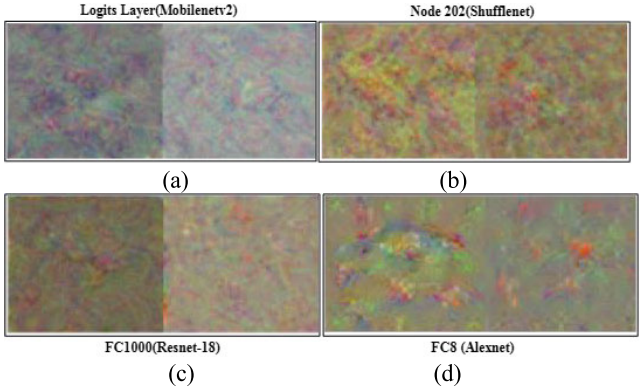

FIGURE 9. Feature learning process on selected layers of transfer learning models (a) mobilenetv2 (b) shuffle net (c) Resnet-18 (d) Alexnet.

TABLE 3. Parameters of NSGA for optimum features selection.

Parameters	Values
Iterations Maximum	20
Size of Population	20
Crossover %	0.7
Offsprings	$2 \times \text{round}(\text{Percentage of Crossover} \times \frac{\text{Population Size}}{2})$
Mutation %	0.4
Mutation Rate	0.1

each model FC8, FC1000, Logits, and node_202 respectively (as shown in Figure 9).

The extracted features are fused serially, and then NSGA is used to choose the best features based on highest scores.

TABLE 4. Datasets related to WBC.

Images without ground truth		
Dataset	**WBC types**	**Number of total images**
LISC	Monocyte	1901
	Neutrophil	2488
	Lymphocyte	2480
	Basophil	54
	Eosinophil	2488
	Mixture	40
ALL-IDB1	blast/non-blast cells	106(33 blast and 74 non-blast)
ALL-IDB2		260(130 blast and 130 non-blast)
Images with ground truth		
LISC	Monocyte	49
	Neutrophil	51
	Lymphocyte	53
	Basophil	54
	Eosinophil	79
	Mixture	9

For the categorization of WBC, the optimized feature vector is supplied to the specified classifiers with 10 fold cross-validation. Figure 10 depicts the feature extraction and categorization stages.

D. OPTIMUM FEATURES SELECTION USING NSGA

NSGA [48] is a probabilistic algorithm used to solve computational problems that might be minimized to find out good

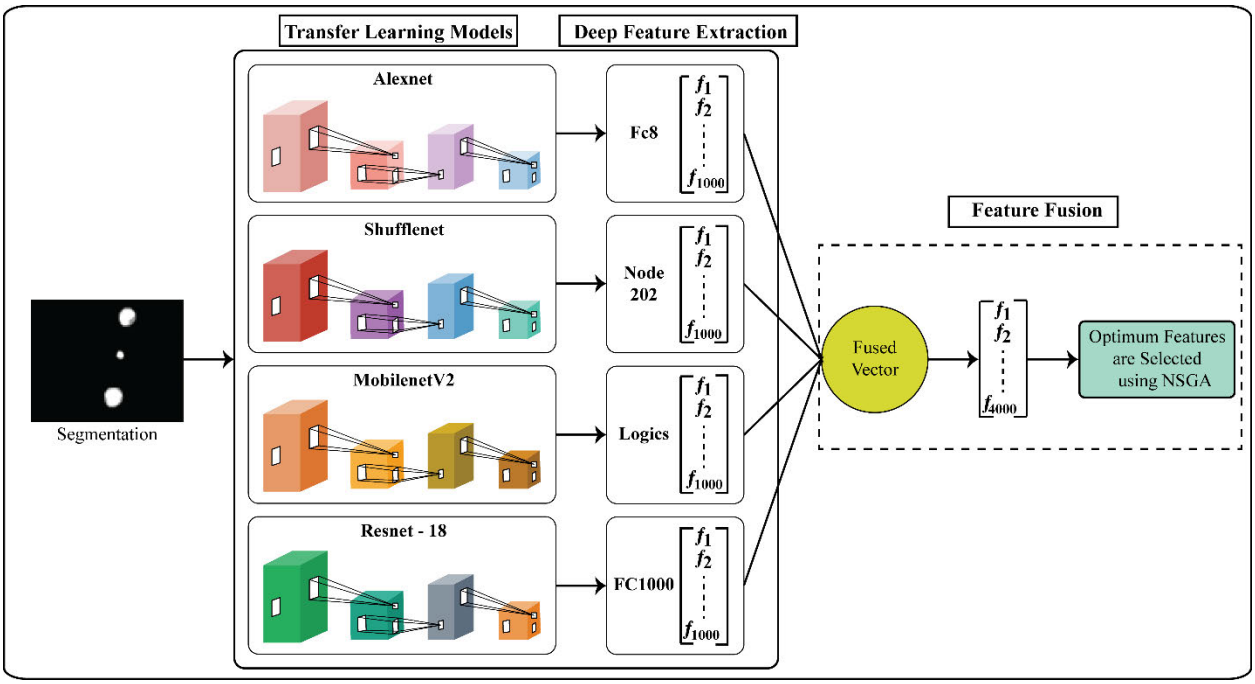

FIGURE 10. Feature extraction, fusion, and selection process.

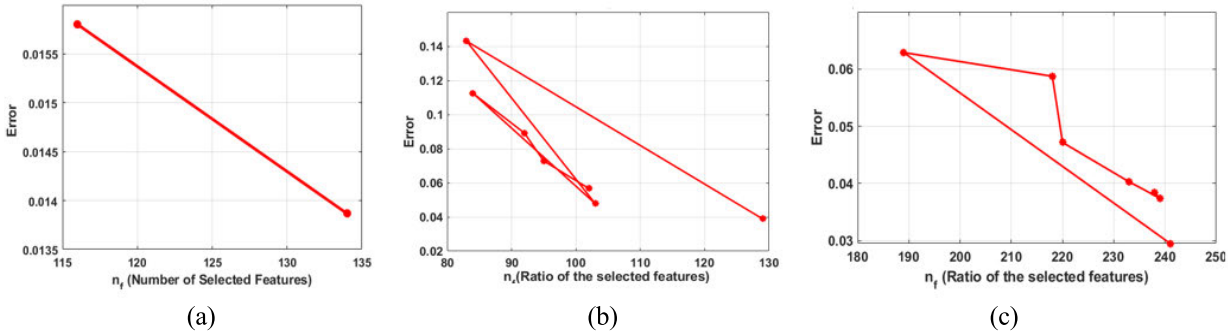

FIGURE 11. NSGA is used to choose the best features (a) ALL-IDB1 (b) ALL-IDB2 (c) LISC.

suitable path by graph. NSGA is used to choose optimum features in which redundant features are reduced and optimum features are selected based on fitness function. Each transfer learning model's 1000 deep features are extracted, and selected features are fused serially. The length of fused vector is N × 4000. The finalized feature vector is sent to NSGA, which chooses the best features. The overall error rate and ratio of selected features from each dataset is shown in Figure 11. Table 3 lists the NSGA parameters.

The overall error rate is minimized, and best cost is 0.01386 on ALL-IDB1, 0.04 on ALL-IDB2 and 0.01386 on LISC dataset. For WBC prediction, the final optimized feature vector is sent to various classifiers. The following is an algorithm for detecting and classifying WBC.

IV. RESULTS AND DISCUSSION

The proposed work is evaluated on Leukocyte image for segmentation and classification (LISC) [49], Acute Lymphoblastic Leukemia Image (ALL_IDB1) and ALL_IDB2 [50]–[53] datasets for the detection and classification of WBC.

The summary of datasets with and without ground truth images is given in Table 4. The proposed method results are computed on MATLAB Toolbox software with 2070 RTX Graphic Card, windows operating system.

A. EXPERIMENT#1 SEGMENTATION OF WBCs

On benchmark datasets, segmentation results are compared to ground truth pixel by pixel in this investigation. Figure 12 shows the LISC dataset segmentation results with ground truth.

The segmentation results are measured pixel by pixel with ground truth in terms of different measures such as dice and Jaccard index. Maximum dice score is 0.9515 and minimum Jaccard distance is 0.0924. Figure 13-14

Algorithm 1 Segmentation and Classification of WBC

Input: WBCimage $\phi(x, y)$
Output: Different types of WBC $\psi(x, y)$
Begin
  for i $\leftarrow$ 1 to Max Images ***do***
    $\phi_{\text{HSV}}(x, y) \leftarrow \phi(x, y)$
    $\phi_{\text{saturation channel}}(x, y) \leftarrow \phi(x, y)$ $\therefore$ Thresholding Method 2 on saturation channel
    $\phi_{T1}(x, y) \leftarrow \phi_{\text{saturation channel}}(x, y)$ $\therefore$ Thresholding Method 1
    $\Phi_{o1}(x, y) \leftarrow \phi_{T1}(x, y)$ $\therefore$ Morphological opening with 8 disc shape structuring element
    $\phi_{T2}(x, y) \leftarrow \phi_{\text{saturation channel}}(x, y)$ $\therefore$ Thresholding Method 2 on saturation channel
    $\phi_{o2}(x, y) \leftarrow \phi_{T2}(x, y)$ $\therefore$ Morphological opening with 28 disc shape structuring element
    $[\phi_{o1}(x, y) + \phi_{o2}(x, y)] \leftarrow \phi_{\text{Parallel Fusion}}(x, y)$ $\therefore$ Parallel fusion of Thresholding Method 1and Thresholding Method 2
    for j $\leftarrow$ 1 to Max Features ***do***
      $[\phi_{o1}(x, y) + \phi_{o2}(x, y)] \leftarrow$ Deep features extracted using shufflenet, mobilenetv2, Alexnet and Resnet $-$ 18
      Deep features extracted are fused shufflenet+mobilenetv2+Alexnet + Resnet-18 $\leftarrow FV$
      FV $\leftarrow$ NSGA $\therefore$ Features Optimization using NSGA
    end for
    NB, DT, Ensemble, LDA, KNN
    $\psi(x, y) \leftarrow$ Classificationofdifferent types of WBC
  end for
end

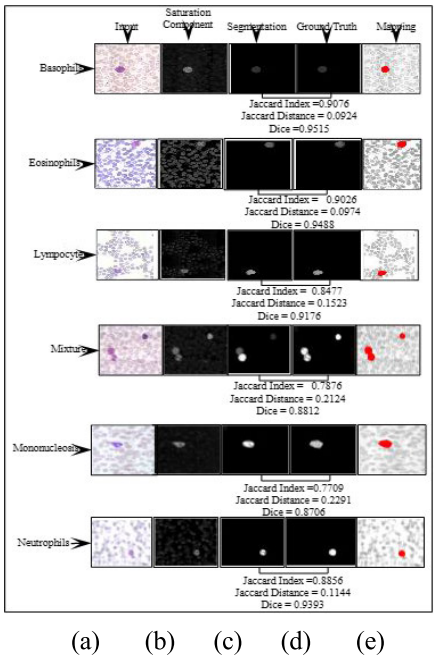

FIGURE 12. Segmented WBC with ground truth (a) input (b) segmented region (c) ground truth (d) mapping.

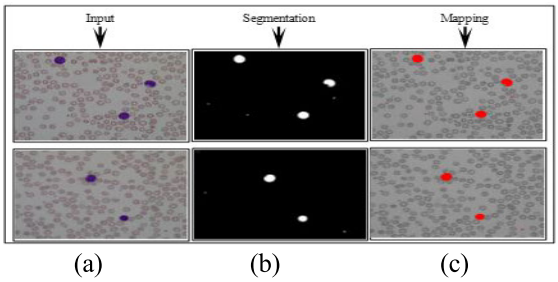

FIGURE 13. Segmented WBC on ALL_IDB1 dataset (a) input (b) segmentation (c) segmentation mapped on input (red highlighted).

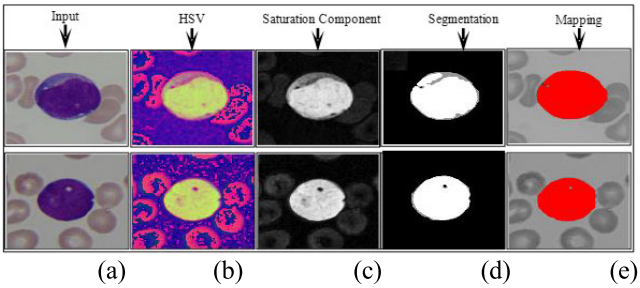

FIGURE 14. Segmentation results on ALL_IDB2 dataset (a) input (b) HSV color space (c) saturation component (d) segmentation (e) segmentation mapping on input.

shows the segmentation results for the ALL IDB1&2 datasets.

B. EXPERIMENT#2 CLASSIFICATION

In this experiment, classification is performed using optimized feature vector. The results are computed to classify the blast/non-blast cells as well as different types of WBC.

The classification of blast/non-blast cells are presented from Table 5-7 on ALL_IDB1 dataset and Table 8-10 on ALL_IDB2 dataset while graphical results in terms of ROCs are also presented in Figure 15 on ALL_IDB1 dataset and Figure 16 on ALL_IDB2 dataset. The classification results

TABLE 5. Classification results using features fusion (Resnet-18 and mobilenetv2) on ALL_IDB1.

Classifier	TP	TN	FP	FN	SE	SP	FPR	FNR	PPV	NPV	ACC	AUC
NB	74	31	0	2	0.9737	1.00	0.00	0.0263	1.00	0.9394	0.9813	0.9992
DT	71	33	3	0	1.00	0.9167	0.0833	0.00	0.9595	1.00	0.9720	0.9828
Ensemble	72	9	2	24	0.7500	0.8182	0.1818	0.2500	0.9730	0.2727	0.7570	0.8953
LDA	74	33	0	0	1.00	1.00	1.00	0.00	0.00	1.00	1.00	1.00
KNN	74	33	0	0	1.00	1.00	1.00	0.00	0.00	1.00	1.00	1.00

TABLE 6. Classification results on ALL_IDB1 using fusion of deep features (mobilenetv2 and shuffle net).

Classifier	TP	TN	FP	FN	SE	SP	FPR	FNR	PPV	NPV	ACC	AUC
NB	69	29	5	4	0.9452	0.8529	0.1471	0.0548	0.9324	0.8788	0.9159	0.9603
DT	74	32	0	1	0.9867	1.00	0.00	0.0133	1.00	0.9697	0.9907	0.9988
Ensemble	67	10	4	26	0.7204	0.7143	0.2857	0.2796	0.9437	0.2778	0.7196	0.7331
LDA	64	21	10	12	0.8421	0.6774	0.3226	0.1579	0.8649	0.6364	0.7944	0.8915
KNN	74	33	0	0	1.00	1.00	1.00	0.00	0.00	1.00	1.00	1.00

TABLE 7. Classification of blast/non-blast cells on ALL_IDB1using fusion of Alex, Shuffle, mobile, and Resnet-18 features.

Classifier	TP	TN	FP	FN	SE	SP	FNR	FPR	PPV	NPV	ACC	AUC
NB	70	28	4	5	0.9333	0.8750	0.0667	0.1250	0.9459	0.8485	0.9159	0.9746
DT	73	31	1	2	0.9733	0.9688	0.0267	0.0313	0.9865	0.9394	0.9720	0.9963
Ensemble	71	9	3	24	0.7474	0.7500	0.2526	0.2500	0.9595	0.2727	0.7477	0.8243
LDA	66	20	8	13	0.8354	0.7143	0.1646	0.2857	0.8919	0.6061	0.8037	0.8776
KNN	74	33	0	0	1.00	1.00	1.00	0.00	0.00	1.00	1.00	1.00

TABLE 8. Classification results using fusion of Resnet-18 and mobilenetv2 features on ALL_IDB2 dataset.

Classifier	TP	TN	FP	FN	SE	SP	FNR	FPR	PPV	NPV	ACC	AUC
NB	130	109	21	0	1.00	0.8385	0.00	0.1615	0.8609	1.00	0.9192	0.9115
DT	128	127	2	3	0.9771	0.9845	0.0229	0.0155	0.9846	0.9769	0.9808	0.9989
Ensemble	123	57	7	73	0.6276	0.8906	0.3724	0.1094	0.9462	0.4385	0.6923	0.9458
LDA	76	64	54	66	0.5352	0.5424	0.4648	0.4576	0.5846	0.4923	0.5385	0.5754
KNN	130	130	0	0	1.00	1.00	1.00	0.00	0.00	1.00	1.00	1.00

TABLE 9. Classification results using the fusion of mobilenetv2 and shuffle net features on ALL_IDB2 dataset.

Classifier	TP	TN	FP	FN	SE	SP	FNR	FPR	PPV	NPV	ACC	AUC
NB	18	130	112	0	1.00	0.5372	0	0.4628	0.1385	1.00	0.5692	0.9417
DT	127	127	3	3	0.9769	0.9769	0.0231	0.0231	0.9769	0.9769	0.9769	0.9983
Ensemble	114	38	16	92	0.5534	0.7037	0.4466	0.2963	0.8769	0.2923	0.5846	0.7844
LDA	130	130	0	0	1.00	1.00	1.00	0.00	0.00	1.00	1.00	1.00
KNN	130	130	0	0	1.00	1.00	1.00	0.00	0.00	1.00	1.00	1.00

are analyzed by the fusion of deep features extracted through different combinations of transfer learning models such as (i) Resnet-18 and mobilenetv2, results are presented in Table 5. (ii) Mobilenetv2 and shuffle net, results are presented in Table 6, and (iii) Resnet-18, mobilenetv2, shuffle net, and Alexnet in Table 6 on ALL_IDB1 dataset.

The results in Table 5 show that LDA and KNN achieved an accuracy of 1.00 while 0.9813 on NB, 0.9720 on decision tree, and 0.7570 on ensemble classifiers is obtained.

From the results in Table 6, maximum accuracy is 1.00 and 0.9907 obtained on KNN and DT classifiers respectively.

TABLE 10. Classification results using ALL_IDB2 dataset (fusion of Alexnet, Resnet-18, shuffle net, and mobilenetv2).

Classifier	TP	TN	FP	FN	SE	SP	FNR	FPR	PPV	NPV	ACC	AUC
NB	110	130	20	0	1.00	0.8667	0.00	0.1333	0.8462	1.00	0.9231	0.9930
DT	126	125	4	5	0.9618	0.9690	0.0382	0.0310	0.9692	0.9615	0.9654	0.9961
Ensemble	112	53	18	77	0.5926	0.7465	0.4074	0.2535	0.8615	0.4077	0.6346	0.8622
LDA	130	130	0	0	1.00	1.00	0.00	0.00	1.00	1.00	1.00	1.00
KNN	130	130	0	0	1.00	1.00	0.00	0.00	1.00	1.00	1.00	1.00

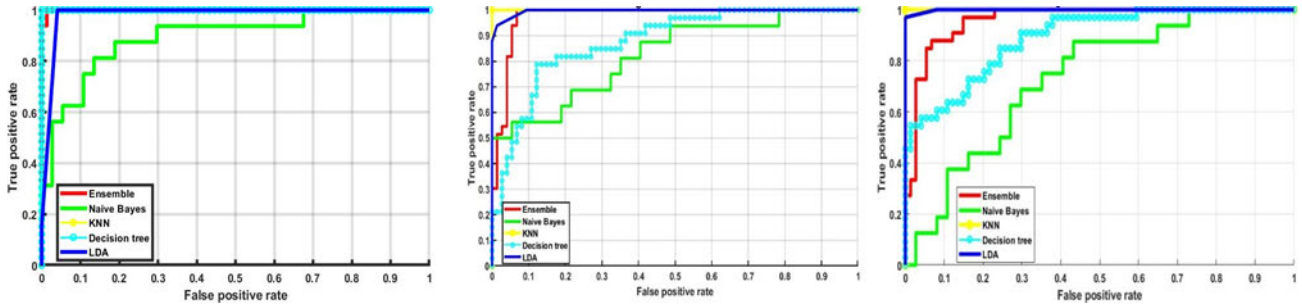

FIGURE 15. (a) Resnet-18 and mobilenetv2 features (b) mobilenetv2 and shuffle net s (c) Alex, Resnet-18, shuffle and mobilenetv2 features.

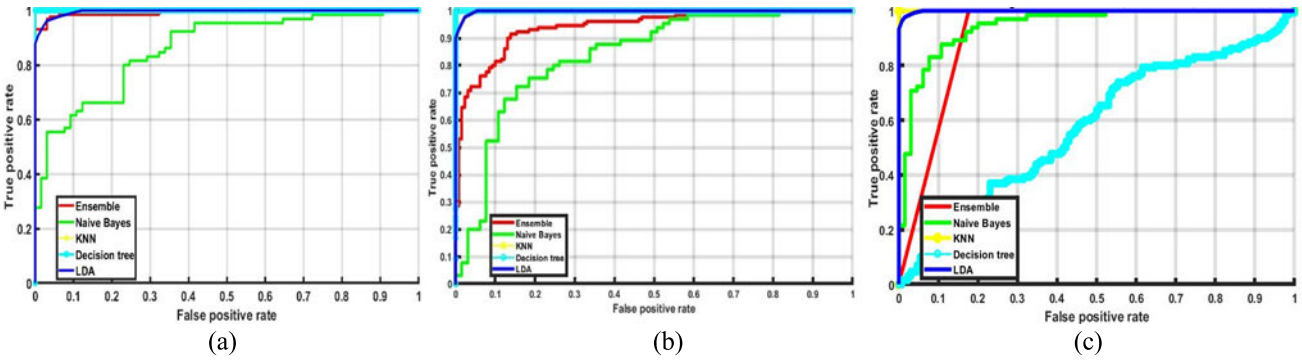

FIGURE 16. Classification results on fusion of Resnet-18 and mobilenetv2 features (b) Alex net, Resnet-18, mobilenetv2, shuffle net (c) shuffle net and mobilev2net.

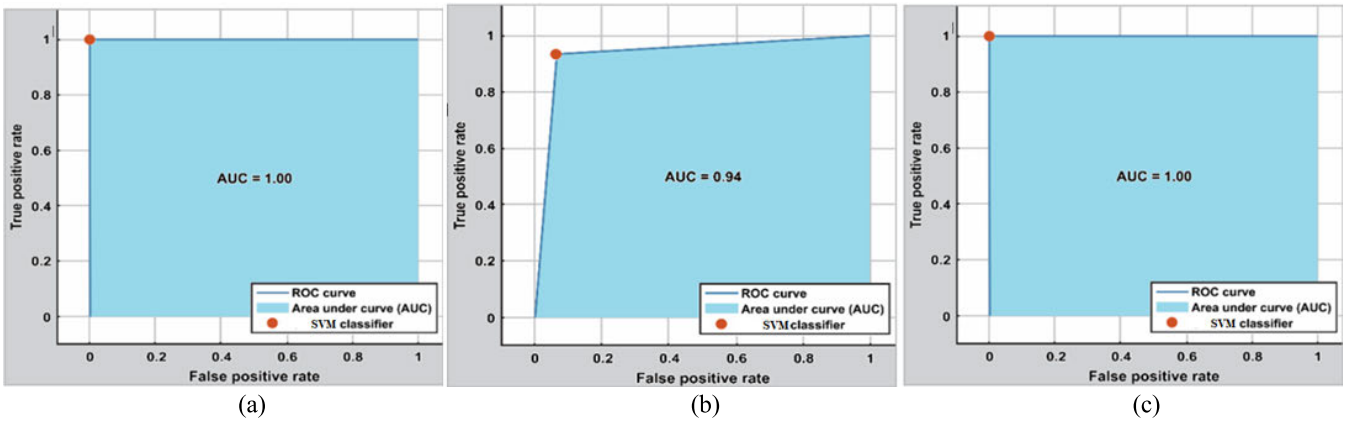

FIGURE 17. ROC on the fusion of deep features (a) mobilenetv2 and shuffle net features (b) mobilenetv2 and Resnet-18 features (c) mobilenetv2 and shuffle net, Alex and Resnet-18 features.

Similarly, 0.9159 is on NB, 0.7196 on ensemble and 0.7944 on LDA classifier.

In Table 7, the results shows that accuracy obtained on KNN and DT are 1.00 and 0.9720 respectively which are maximum as compared to other classifiers mentioned in the same table.

Overall results from Table 5-7 show that [Resnet-18 and mobilenetv2] achieved maximum accuracy as

TABLE 11. Classification results with SVM using a fusion of mobilenetv2 and Resnet-18 features on LISC dataset.

Types of WBC	SE	SP	FNR	FPR	PPV	NPV	ACC
Basophil	0.9936	0.9936	0.0064	0.0064	0.9936	0.9936	0.9936
Eosinophil	0.9659	0.9767	0.0341	0.0233	0.9733	0.9702	0.9717
Mixture	1.00	0.9882	0.00	0.0118	0.9865	1.00	0.9937
Monocyte	0.9623	0.9882	0.0377	0.0118	0.9865	0.9671	0.9760
Neutrophil	0.9961	0.9800	0.0039	0.0200	0.9770	0.9966	0.9874
Lymphocyte	0.9961	0.9983	0.0039	0.0017	0.9980	0.9966	0.9973

TABLE 12. Classification results using fusion of mobilenetv2 and shuffle net features on LISC dataset.

Types of WBC	SE	SP	FNR	FPR	PPV	NPV	ACC
Basophil	0.9872	0.9888	0.0128	0.0112	0.9888	0.9873	0.9880
Eosinophil	0.9904	0.9904	0.0096	0.0096	0.9904	0.9904	0.9904
Mixture	0.9984	0.9984	0.0016	0.0016	0.9984	0.9984	0.9984
Monocyte	1.00	0.9084	0.00	0.0017	0.9904	1.00	0.9902
Neutrophil	0.9936	0.9936	0.0064	0.0064	0.9936	0.9936	0.9936
Lymphocyte	1.00	0.9984	0.00	0.0016	0.9984	1.00	0.9990

TABLE 13. Classification results using the fusion of mobilenetv2 and shuffle net, Alex and Resnet-18 features on LISC dataset.

Types of WBC	SE	SP	FNR	FPR	PPV	NPV	ACC
Basophil	1.00	0.9984	0.00	0.0016	0.9984	1.00	0.9992
Eosinophil	1.00	1.00	0.00	0.00	1.00	1.00	1.00
Mixture	1.00	1.00	0.00	0.00	1.00	1.00	1.00
Monocyte	1.00	1.00	0.00	0.00	1.00	1.00	1.00
Neutrophil	1.00	1.00	0.00	0.00	1.00	1.00	1.00
Lymphocyte	1.00	1.00	0.00	0.00	1.00	1.00	1.00

compared to [shuffle net and mobilenetv2] and [Alex net, Resnet-18, mobilenetv2, shuffle net] transfer learning models.

The classification results are evaluated on ALL_IDB2 database based on the fusion of deep features with different combinations i.e., (i) Resnet-18 and mobilenetv2, Table 8 summarizes the findings (ii) Mobilenetv2 and shuffle net, results are given in Table 9, and (iii) Resnet-18, mobilenetv2, shuffle net and Alexnet whose results are shown in Table 10. The ROCs are also presented in Figure 16.

In Table 8, maximum accuracy is 1.00 with KNN and 0.9808 with DT tree is obtained. While accuracy with LDA is 0.5385, 0.6923 is with ensemble and 0.9192 with NB is obtained.

The results in Table 9 show that 0.5846 accuracy achieved on ensemble, 0.5692 on NB, 0.9769 on decision tree and 1.00 on LDA and KNN classifiers.

Results in Table 10 show that KNN and LDA obtained an accuracy of 1.00 while ensemble showed 0.6346.

Overall results from Table 8-10 show that [Alex net, Resnet-18, mobilenetv2, shuffle net] achieved maximum accuracy as compared to [Resnet-18 and mobilenetv2] and [shuffle net and mobilenetv2] transfer learning models.

TABLE 14. Proposed method computational time.

Proposed Method Steps	Computational Time
Preprocessing	10 minutes and 1 seconds
Segmentation	11 minutes and 6 seconds
Features extraction	16 minutes and 3 seconds
Classification	18 minutes and 2 seconds

C. EXPERIMENT#3 CLASSIFICATION OF WBCs

In this experiment, results are computed to classify different types of blood cells using SVM classifier. WBC's classification results are derived on the LISC dataset using a fusion of deep features gathered using various transfer learning methods, such as (i) mobilenetv2 and Resnet-18 (ii) mobilenetv2 and shuffle net, and (iii) mobilenetv2 and shuffle net, Alex and Resnet-18 through SVM classifier with the cubic kernel. The results are presented from Table 11-13 and graphically in terms of ROC in Figure 17.

In Table 11, results in terms of accuracy obtained are, 0.9936 on Basophil, 0.9717 on Eosinophil, 0.9874 on Neutrophil and 0.9973 on Lymphocyte cells.

The results in Table 12 show that maximum 0.9990 accuracy is achieved on Lymphocyte while 0.9880 on Basophil.

TABLE 15. Comparison of proposed with existing methodologies.

Ref	Year	Dataset	Classification	Results
[9]	2020	ALL-IDB2	Blast/non-blast cell	98.61 ACC, 99.33 SE
[56]	2021			0.98.02 ACC
[57]	2020	ALL-IDB1		0.97184 ACC
Proposed method		ALL-IDB1&2		1.00 ACC
				1.00 ACC
[58]	2020	LISC	Lymphocyte Monocyte Basophil Eosinophil Neutrophil	0.9952 0.9840 0.9848 0.9616 0.9504
[59]	2019			Overall, 0.973ACC
[56]	2021			0.9858 ACC
Proposed method				0.9992 1.00 1.00 1.00 1.00 1.00

The results in Table 13 demonstrate that accuracy is 0.9992 on Basophil while 1.00 on all others cell types such as Eosinophil, Mixture, Monocyte, Neutrophil, and Lymphocyte. The overall results in Table 11-13 show that [mobilenetv2 and shuffle net, Alex and Resnet-18] perform better as compared to [Resnet-18 and mobilenetv2] and [shuffle net and mobilenetv2] transfer learning models.

Table 14 shows the computational cost/time of the proposed approach.

Table 15 compares the proposed method's results to the most recent current techniques.

In Table 15, results are compared with existing methods on the same benchmark datasets for similar types of WBC. The comparison demonstrates that the proposed strategy outperformed the most recent work in this domain.

V. CONCLUSION

The work given here detects and classifies many types of WBC as well as leukemia. The three key operations in the technique are segmentation, feature extraction, and classification. Mobilenetv2 and Resnet-18 outperform the fusion of other feature vectors in the categorization of blast/non-blast cells on ALL IDB1& 2, respectively. Finally, it is observed that DT classifies blast and non-blast cells more accurately. Similarly, feature vector obtained the maximum accuracy utilizing SVM to classify different types of blood cells on the fusion of Alexnet, shuffle net, mobilenetv2 and Resnet-18. Finally, study concludes that the proposed strategy produces better outcomes than existing methods. This approach could be expanded to recognize blood cells on real patient data in the future, reducing haematologists' burden.

REFERENCES

[1] L. N. Castro, L. N. De Castro, and J. Timmis, *Artificial Immune Systems: A New Computational Intelligence Approach*. Canterbury, U.K.: Springer, 2002

[2] L. Gustafsson, D. Nordling, M. Andersson, and B. Sheldon, "Infectious diseases, reproductive effort and the cost of reproduction in birds," *Phil. Trans. Roy. SoC. London. Ser. B, Biol. Sci.*, vol. 346, no. 1317, pp. 323–331, 1994.

[3] T. Rademakers, M. Goedhart, M. Hoogenboezem, A. G. Ponce, J. Van Rijssel, M. Samus, M. Schnoor, S. Butz, S. Huveneers, D. Vestweber, M. A. Nolte, C. Voermans, and J. D. van Buul, "Hematopoietic stem and progenitor cells use podosomes to transcellularly cross the bone marrow endothelium," *Haematologica*, vol. 105, no. 12, pp. 2746–2756, Jan. 2020.

[4] N. Verma, M. Liu, H. Ly, A. Loria, K. S. Campbell, H. Bush, P. A. Kern, P. A. Jose, H. Taegtmeyer, D. M. Bers, S. Despa, L. B. Goldstein, A. J. Murray, and F. Despa, "Diabetic microcirculatory disturbances and pathologic erythropoiesis are provoked by deposition of amyloid-forming amylin in red blood cells and capillaries," *Kidney Int.*, vol. 97, no. 1, pp. 143–155, Jan. 2020.

[5] A. G. Freifeld and D. R. Kaul, "Infection in the patient with cancer," in *Abeloff's Clinical Oncology*. Amsterdam, The Netherlands: Elsevier, 2020, pp. 544–564.

[6] J. Amin, M. Sharif, M. Raza, T. Saba, and M. A. Anjum, "Brain tumor detection using statistical and machine learning method," *Comput. Methods Programs Biomed.*, vol. 177, pp. 69–79, Aug. 2019.

[7] H. L. Malech, F. R. DeLeo, and M. T. Quinn, "The role of neutrophils in the immune system: An overview," in *Neutrophil*. New York, NY, USA: Humana, 2020, pp. 3–10.

[8] C. Chakraborty, B. Gupta, and S. K. Ghosh, "Mobile telemedicine systems for remote patient's chronic wound monitoring," in *Virtual Mobile Healthcare: Breakthroughs Research Practice*. Hershey, PA, USA: IGI Global, 2020, pp. 977–1003.

[9] P. P. Banik, R. Saha, and K.-D. Kim, "An automatic nucleus segmentation and CNN model based classification method of white blood cell," *Expert Syst. Appl.*, vol. 149, Jul. 2020, Art. no. 113211.

[10] Y. Yang, Q. Huang, C. Luo, Y. Wen, R. Liu, H. Sun, and L. Tang, "MicroRNAs in acute pancreatitis: From pathogenesis to novel diagnosis and therapy," *J. Cellular Physiol.*, vol. 235, no. 3, pp. 1948–1961, Mar. 2020.

[11] N. Singh and B. Tripathy, "Leukemia cell segmentation from microscopic blood smear image using C-mode," in *Soft Computing for Problem Solving*. Singapore: Springer, 2020, pp. 225–238.

[12] G. Bueno, M. M. Fernandez-Carrobles, L. Gonzalez-Lopez, and O. Deniz, "Glomerulosclerosis identification in whole slide images using semantic segmentation," *Comput. Methods Programs Biomed.*, vol. 184, Feb. 2020, Art. no. 105273.

[13] K. K. Jha and H. S. Dutta, "Nucleus and cytoplasm–based segmentation and actor-critic neural network for acute lymphocytic leukaemia detection in single cell blood smear images," *Med. Biol. Eng. Comput.*, vol. 58, no. 1, pp. 171–186, Jan. 2020.

[14] Y. Li, R. Zhu, L. Mi, Y. Cao, and D. Yao, "Segmentation of white blood cell from acute lymphoblastic leukemia images using dual-threshold method," *Comput. Math. Methods Med.*, vol. 2016, pp. 1–12, Jun. 2016.

[15] A. C. Hauptfleisch, "Automatic road network extraction from high resolution satellite imagery using spectral classification methods," Ph.D. dissertation, Univ. Pretoria, Pretoria, South Africa, 2010.

[16] V. Rajinikanth, N. Madhavaraja, S. C. Satapathym, S. Chandra, and S. L. Fernandes, "Otsu's multi-thresholding and active contour snake model to segment dermoscopy images," *J. Med. Imag. Health Inform.*, vol. 7, no. 8, pp. 1837–1840, 2017.

[17] N. Nida, M. Sharif, M. U. G. Khan, M. Yasmin, and S. L. J. I. J. Fernandes, "A framework for automatic colorization of medical imaging," *IIOAB J.*, vol. 7, pp. 202–209, Jan. 2016.

[18] B. C. Ko, J.-W. Gim, and J.-Y. Nam, "Automatic white blood cell segmentation using stepwise merging rules and gradient vector flow snake," *Micron*, vol. 42, no. 7, pp. 695–705, Oct. 2011.
[19] A. Boucher and C. Garbay, "A multi-agent system to segment living cells," in *Proc. 13rd Int. Conf. Pattern Recognit.*, 1996, pp. 558–562.
[20] H. T. Madhloom, S. A. Kareem, and H. Ariffin, "An image processing application for the localization and segmentation of lymphoblast cell using peripheral blood images," *J. Med. Syst.*, vol. 36, no. 4, pp. 2149–2158, Aug. 2012.
[21] J. Amin, M. Sharif, M. Yasmin, and S. L. Fernandes, "A distinctive approach in brain tumor detection and classification using MRI," *Pattern Recognit. Lett.*, vol. 139, pp. 118–127, Nov. 2020.
[22] S. M. Naqi, M. Sharif, M. Yasmin, and S. L. Fernandes, "Lung nodule detection using polygon approximation and hybrid features from CT images," *Current Med. Imag. Rev.*, vol. 14, no. 1, pp. 108–117, Dec. 2017.
[23] A. Rehman, N. Abbas, T. Saba, S. I. U. Rahman, Z. Mehmood, and H. Kolivand, "Classification of acute lymphoblastic leukemia using deep learning," *Microsc. Res. Technique*, vol. 81, no. 11, pp. 1310–1317, Nov. 2018.
[24] V. Rajinikanth, S. C. Satapathy, S. L. Fernandes, and S. Nachiappan, "Entropy based segmentation of tumor from brain MR images—A study with teaching learning based optimization," *Pattern Recognit. Lett.*, vol. 94, pp. 87–95, Jul. 2017.
[25] V. Rajinikanth, S. L. Fernandes, B. Bhushan, and N. R. Sunder, "Segmentation and analysis of brain tumor using Tsallis entropy and regularised level set," in *Proc. 2nd Int. Conf. Micro-Electron., Electromagn. Telecommun.* Singapore: Springer, 2018, pp. 313–321.
[26] S. T. Fatima Bokhari, M. Sharif, M. Yasmin, and S. L. Fernandes, "Fundus image segmentation and feature extraction for the detection of glaucoma: A new approach," *Current Med. Imag. Rev.*, vol. 14, no. 1, pp. 77–87, Dec. 2017.
[27] S. Mohapatra and D. Patra, "Automated leukemia detection using Hausdorff dimension in blood microscopic images," in *Proc. INTERACT*, 2010, pp. 64–68.
[28] G. Nyamundanda, L. Brennan, and I. C. Gormley, "Probabilistic principal component analysis for metabolomic data," *BMC Bioinf.*, vol. 11, no. 1, p. 571, Dec. 2010.
[29] K. G. Dhal, J. Gálvez, S. Ray, A. Das, and S. Das, "Acute lymphoblastic leukemia image segmentation driven by stochastic fractal search," *Multimedia Tools Appl.*, vol. 2020, pp. 1–29, Jan. 2020.
[30] P. Sukumar and R. K. Gnanamurthy, "Segmentation and abnormality detection of cervical cancer cells using fast elm with particle swarm optimization," *Genetika*, vol. 47, no. 3, pp. 863–876, 2015.
[31] G. Gaipa, G. Basso, A. Biondi, and D. Campana, "Detection of minimal residual disease in pediatric acute lymphoblastic leukemia," *Cytometry B, Clin. Cytometry*, vol. 84, no. 6, pp. 359–369, Nov. 2013.
[32] X. Chen, M. Lv, L. Zhao, and X. Zhang, "An improved particle swarm optimization for protein folding prediction," *Int. J. Inf. Eng. Electron. Bus.*, vol. 3, no. 1, pp. 1–8, Feb. 2011.
[33] S. S. Adagale and S. S. Pawar, "Image segmentation using PCNN and template matching for blood cell counting," in *Proc. IEEE Int. Conf. Comput. Intell. Comput. Res.*, Dec. 2013, pp. 1–5.
[34] K. S. Tan, N. A. M. Isa, and W. H. Lim, "Color image segmentation using adaptive unsupervised clustering approach," *Appl. Soft Comput.*, vol. 13, no. 4, pp. 2017–2036, Apr. 2013.
[35] M. Sharif, J. Amin, M. Yasmin, and A. Rehman, "Efficient hybrid approach to segment and classify exudates for DR prediction," *Multimedia Tools Appl.*, vol. 79, nos. 15–16, pp. 11107–11123, Apr. 2020.
[36] J. Amin, M. Sharif, N. Gul, S. Kadry, and C. Chakraborty, "Quantum machine learning architecture for COVID-19 classification based on synthetic data generation using conditional adversarial neural network," *Cognit. Comput.*, vol. 14, pp. 1–12, Aug. 2021.
[37] J. Amin, M. Almas Anjum, M. Sharif, S. Kadry, and Y. Nam, "Fruits and vegetable diseases recognition using convolutional neural networks," *Comput., Mater. Continua*, vol. 70, no. 1, pp. 619–635, 2022.
[38] S. Saleem, J. Amin, M. Sharif, M. A. Anjum, M. Iqbal, and S.-H. Wang, "A deep network designed for segmentation and classification of leukemia using fusion of the transfer learning models," *Complex Intell. Syst.*, vol. 2021, pp. 1–16, Jul. 2021.
[39] J. Amin, M. Sharif, M. A. Anjum, H. U. Khan, M. S. A. Malik, and S. Kadry, "An integrated design for classification and localization of diabetic foot ulcer based on CNN and YOLOv2-DFU models," *IEEE Access*, vol. 8, pp. 228586–228597, 2020.
[40] M. Sharif, J. Amin, A. Siddiqa, H. U. Khan, M. S. A. Malik, M. A. Anjum, and S. Kadry, "Recognition of different types of leukocytes using YOLOv2 and optimized Bag-of-Features," *IEEE Access*, vol. 8, pp. 167448–167459, 2020.
[41] N. Otsu, "A threshold selection method from gray-level histograms," *IEEE Trans. Syst., Man, Cybern.*, vol. SMC-9, no. 1, pp. 62–66, Jan. 1979.
[42] BT, Recommendation ITU-R, "Studio encoding parameters of digital television for standard 4: 3 and wide-screen 16: 9 aspect ratios," Int. Radio Consultative Committee Int. Telecommun. Union, Switzerland, CCIR Rep. 624-4, 2011.
[43] A. R. Smith, "Color gamut transform pairs," *ACM Siggraph Comput. Graph.*, vol. 12, no. 3, pp. 12–19, 1978.
[44] O. Russakovsky, "ImageNet large scale visual recognition challenge," *Int. J. Comput. Vis.*, vol. 115, no. 3, pp. 211–252, Dec. 2015.
[45] K. He, X. Zhang, S. Ren, and J. Sun, "Deep residual learning for image recognition," in *Proc. IEEE Conf. Comput. Vis. Pattern Recognit. (CVPR)*, Jun. 2016, pp. 770–778.
[46] M. Sandler, A. Howard, M. Zhu, A. Zhmoginov, and L.-C. Chen, "MobileNetV2: Inverted residuals and linear bottlenecks," in *Proc. IEEE/CVF Conf. Comput. Vis. Pattern Recognit.*, Jun. 2018, pp. 4510–4520.
[47] X. Zhang, X. Zhou, M. Lin, and J. Sun, "ShuffleNet: An extremely efficient convolutional neural network for mobile devices," in *Proc. IEEE/CVF Conf. Comput. Vis. Pattern Recognit.*, Jun. 2018, pp. 6848–6856.
[48] T. M. Hamdani, J.-M. Won, A. M. Alimi, and F. Karray, "Multi-objective feature selection with NSGA II," in *Proc. Int. Conf. Adapt. Natural Comput. Algorithms*. Berlin, Germany: Springer, 2007, pp. 240–247.
[49] S. H. Rezatofighi, K. Khaksari, and H. Soltanian-Zadeh, "Automatic recognition of five types of white blood cells in peripheral blood," in *Proc. Int. Conf. Image Anal. Recognit.* Berlin, Germany: Springer, 2010, pp. 161–172.
[50] R. D. Labati, V. Piuri, and F. Scotti, "All-IDB: The acute lymphoblastic leukemia image database for image processing," in *Proc. 18th IEEE Int. Conf. Image Process.*, Sep. 2011, pp. 2045–2048.
[51] F. Scotti, "Robust segmentation and measurements techniques of white cells in blood microscope images," in *Proc. IEEE Instrum. Meas. Technol. Conf. Proc.*, Dec. 2006, pp. 43–48.
[52] F. Scotti, "Automatic morphological analysis for acute leukemia identification in peripheral blood microscope images," in *Proc. IEEE Int. Conf. Comput. Intell. Meas. Syst. Appl.*, Dec. 2005, pp. 96–101.
[53] V. Piuri and F. Scotti, "Morphological classification of blood leucocytes by microscope images," in *Proc. IEEE Int. Conf. Comput. Intell. Meas. Syst. Appl.*, 2004, pp. 103–108.
[54] T. Hastie, *The Elements of Statistical Learning Data Mining, Inference, and Prediction*. Cham, Switzerland: Springer, 2008.
[55] L. Breiman, J. H. Friedman, and R. A. Olshen, "Stone," in *CJ: Classification and Regression Trees*. Medina, OH, USA: Wadsworth, 1984.
[56] S. Tarek, H. M. Ebied, A. E. Hassanien, and M. F. Tolba, "White blood cells segmentation and classification using swarm optimization algorithms and multilayer perceptron," *Int. J. Sociotechnol. Knowl. Develop.*, vol. 13, no. 2, pp. 16–30, Apr. 2021.
[57] M. Shahzad, A. I. Umar, M. A. Khan, S. H. Shirazi, Z. Khan, and W. Yousaf, "Robust method for semantic segmentation of whole-slide blood cell microscopic images," *Comput. Math. Methods Med.*, vol. 2020, pp. 1–13, Jan. 2020.
[58] H. Kutlu, E. Avci, and F. Özyurt, "White blood cells detection and classification based on regional convolutional neural networks," *Med. Hypotheses*, vol. 135, Feb. 2020, Art. no. 109472.
[59] D. Gupta, J. Arora, U. Agrawal, A. Khanna, and V. H. C. de Albuquerque, "Optimized binary bat algorithm for classification of white blood cells," *Measurement*, vol. 143, pp. 180–190, Sep. 2019.

JAVARIA AMIN received the Ph.D. degree. She is actively involved in research and producing high-quality work on medical image processing, pattern recognition, and computer vision. She has published more than 40 research articles in reputed and prestigious international journals with an accumulated impact factor of more than 150. Her research interests include the detection of anomalies in human body parts using machine learning and powerful deep learning algorithms.

MUHAMMAD SHARIF (Senior Member, IEEE) received the Ph.D. degree. He has worked one year at Alpha Soft U.K.-based software house, in 1995. He is an OCP at Developer Track. He has been in teaching profession, since 1996. He also headed the department, from 2008 to 2011, and achieved the targeted outputs. He is currently an Associate Professor at COMSATS University Islamabad, Wah Campus, Pakistan. He has more than 215 research publications in IF, SCI, and ISI journals as well as in national and international conferences and obtained more than 250 Impact Factor. He has supervised five Ph.D. (CS) and more than 60 M.S. (CS) thesis to date. His research interests include medical imaging, biometrics, computer vision, machine learning, and agriculture plants. He is being awarded with the COMSATS Research Productivity Award (2011–2018). He served as a TPC Member for IEEE FIT 2014–2019. He is currently serving as an Associate Editor for IEEE Access, a guest editor for special issues, and a reviewer for well reputed journals.

MUHAMMAD ALMAS ANJUM is currently a Professor with the College of Electrical and Mechanical Engineering, National University of Sciences and Technology (NUST), Pakistan. He has been a Team Lead in establishing the Center of Excellence Information Technology, College of Electrical and Mechanical Engineering, and served as its first pioneer Head. He also designed and established the Center of Innovation and Entrepreneurship, College of Electrical and Mechanical Engineering. He has also served as the Dean for the Faculty of Computer Sciences, University of Wah, and the Director of Research and Development for the College of Electrical and Mechanical Engineering, NUST. He has completed different projects around the globe. He has evaluated more than ten Ph.D. thesis. His research interests include pattern recognition, security systems (biometrics), and computer vision. Apart of his more than 50 international publications in his area of specialization, he is the author of a book titled *Face Recognition a Challenge in Biometrics: Image Resolution Issues in Face Recognition*. He is a reviewer/a member of more than dozen international technical committees. He is also an Executive Editor of the *UW Journal of Computer Sciences*.

MUSSARAT YASMIN received the M.S. degree in CS from IQRA University, Pakistan, and the Ph.D. degree. She is currently an Assistant Professor at COMSATS University Islamabad, Wah Campus, Pakistan. Her area of specialization is image processing. She has been in education field, since 1993. She has more than 65 research publications in IF, SCI, and ISI journals as well as in national and international conferences. A number of undergraduate projects are complete under her supervision. She is currently supervising five Ph.D. (CS) students and a good number of M.S. students. Her research interests include neural networks, algorithms design and analysis, machine learning, and image processing. She is an active member of the university research group ''Computer Vision and Intelligent Systems.'' She is a Gold Medalist in M.S. degree (CS) from IQRA University. She is getting COMSATS Research Productivity Award, since 2012.

KHALID IQBAL KHATTAK received the B.Sc. degree from the University of the Punjab, Lahore, the M.S. degree in CS from SZABIST, Karachi, and the Ph.D. degree in applied computer technology from the University of Science and Technology Beijing, in 2014. He is currently an Assistant Professor with the Department of Computer Science, COMSATS University Islamabad, Attock Campus. He is also the Director of the Pattern Recognition, Images and Data Engineering (PRIDE) Research Group, where graduate students are working under his supervision in different fields, such as data mining, social networks, image processing, and deep learning models. He has worked on Bayesian network application for privacy preserving of XML association rules and text localization in scene images. His research work has been published in reputed international conference proceedings and top ranked journals. His research interests include pattern recognition, machine leaning, data mining, and social networks. He was awarded a fully funded scholarship by the China Scholarship Council for the entire duration of his Ph.D. studies. He also won the Excellent Researcher (or excellent international research student award) from the University of Science and Technology Beijing, in from 2012 to 2013. He was a recipient of the CSC scholarship and QCRI/Boeing Travel Grant.

SEIFEDINE KADRY (Senior Member, IEEE) received the bachelor's degree from Lebanese University, in 1999, the dual M.S. degree from Reims University, France, and EPFL, Lausanne, in 2002, the Ph.D. degree from Blaise Pascal University, France, in 2007, and the H.D.R. degree from Rouen University, in 2017. He is an ABET Program Evaluator for computing and ABET Program Evaluator for engineering tech. His research interests include data science, education using technology, system prognostics, stochastic systems, and applied mathematics.

SANGHYUN SEO received the B.S. degree in computer science and engineering from Chung-Ang University, Seoul, South Korea, in 1998, and the M.S. and Ph.D. degrees from the GSAIM Department, Chung-Ang University, in 2000 and 2010, respectively. He was a Senior Researcher with G-Inno System, from 2002 to 2005. He was a Postdoctoral Researcher with Chung-Ang University, in 2010, and the LIRIS Laboratory, Lyon 1 University, from February 2011 to February 2013. He had worked at the Electronics and Telecommunications Research Institute (ETRI), Daejeon, South Korea, from May 2013 to February 2016. He had worked at Sungkyul University, from March 2016 to February 2019. He is currently a Faculty Member with the College of Art and Technology, Chung-Ang University. His research interests include computer graphics, non-photorealistic rendering and animation, real-time rendering using GPU, VR/AR, and game technology. He has been a Reviewer in *Multimedia Tools and Applications* (MTAP), *Computer and Graphics* (Elsevier), U.K., the *Journal of Supercomputing* (JOS), and *Visual Computer* (Springer). He has been a program committee member in many international conferences and workshops. He has edited a number of international journal special issues as a Guest Editor, such as the *Journal of Real-Time Image Processing*, the *Journal of Internet Technology*, and *Multimedia Tools and Applications*. He has been an Associate Editor of the *Journal of Real-Time Image Processing*, since 2017.